

Supplementary Information

5

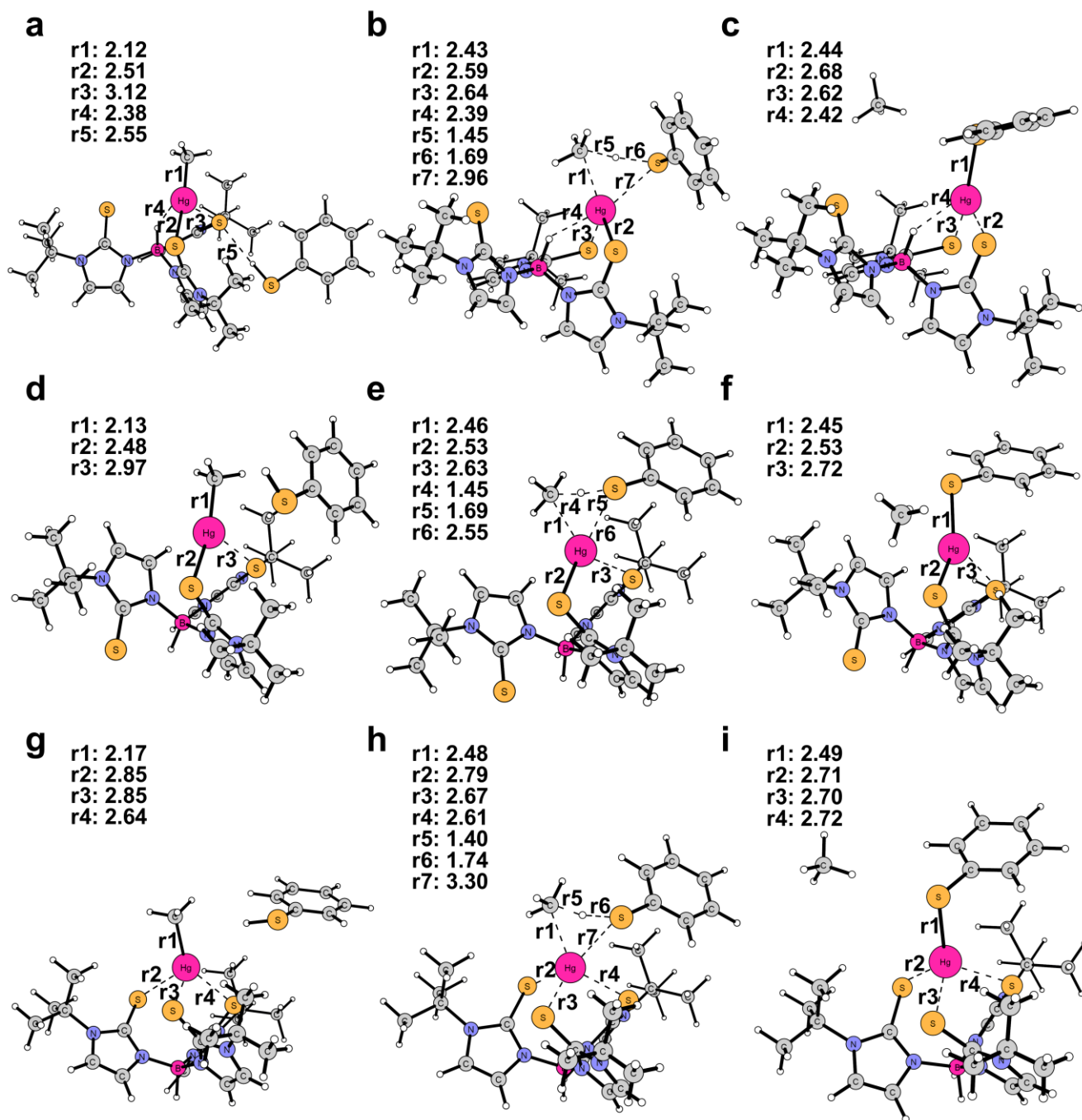


Fig. 1 Structures of the frontside attack pathway featuring four-center TS. (a), (d), and (g): RE for $[\kappa^1/\kappa^2/\kappa^3\text{-Tm}^t\text{-Bu}]\text{HgMe}$ complexes, respectively. (b), (e), and (h): the corresponding TS. (c), (f), and (i): the corresponding PRO.

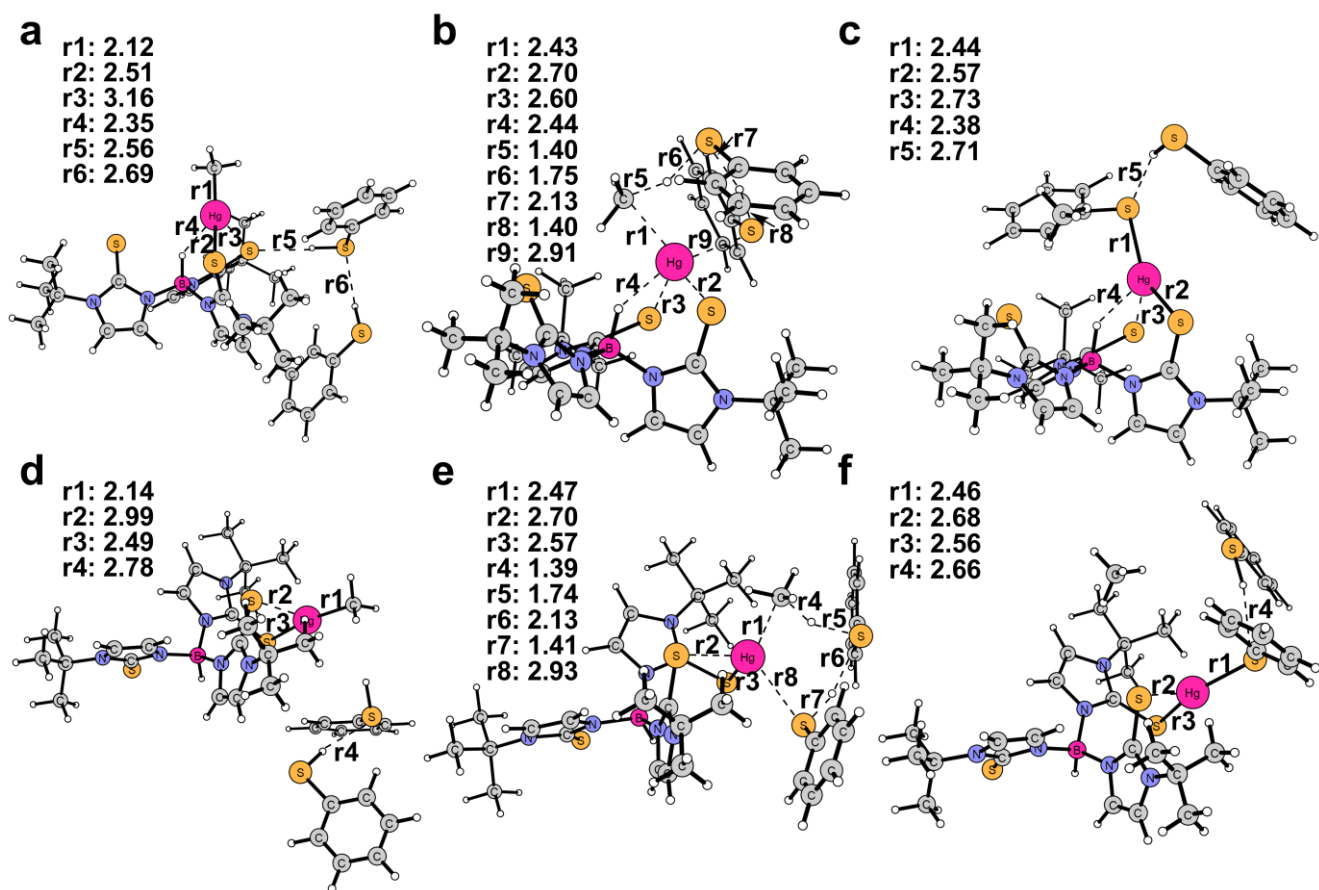


Fig. 2 Structures of the frontside attack pathway featuring six-center TS. (a), (d), and (g): RE for $[\kappa^1/\kappa^2\text{-Tm}^{t\text{-Bu}}]\text{HgMe}$ complexes, respectively. (b), (e), and (h): the corresponding TS. (c), (f), and (i): the corresponding PRO.

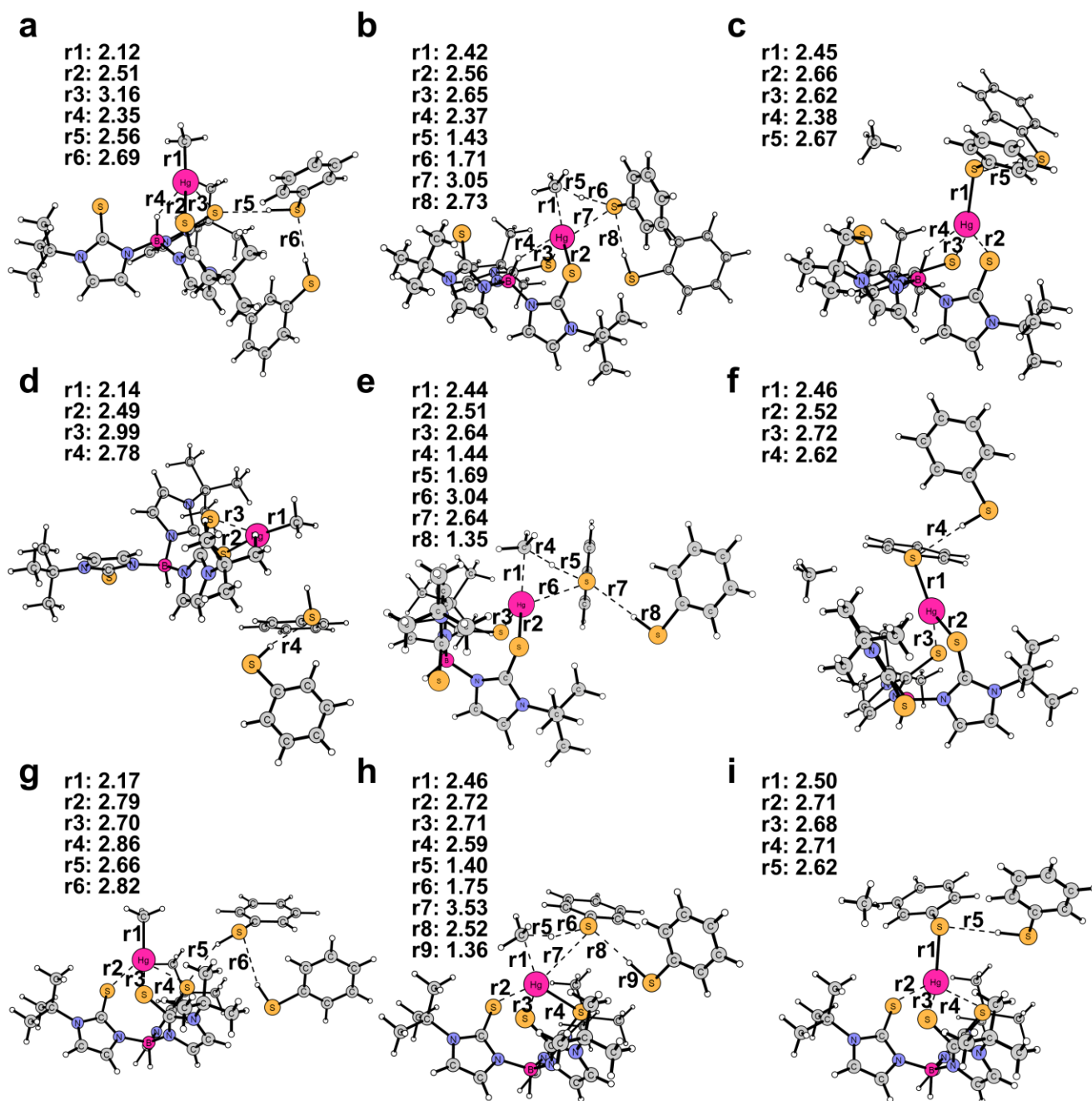


Fig. 3 Structures of the frontside attack pathway featuring HB-assisted four-center TS. (a), (d), and (g): RE for $[\kappa^1/\kappa^2/\kappa^3\text{-Tm}^{\text{t-Bu}}]\text{HgMe}$ complexes, respectively. (b), (e), and (h): the corresponding TS. (c), (f), and (i): the corresponding PRO.

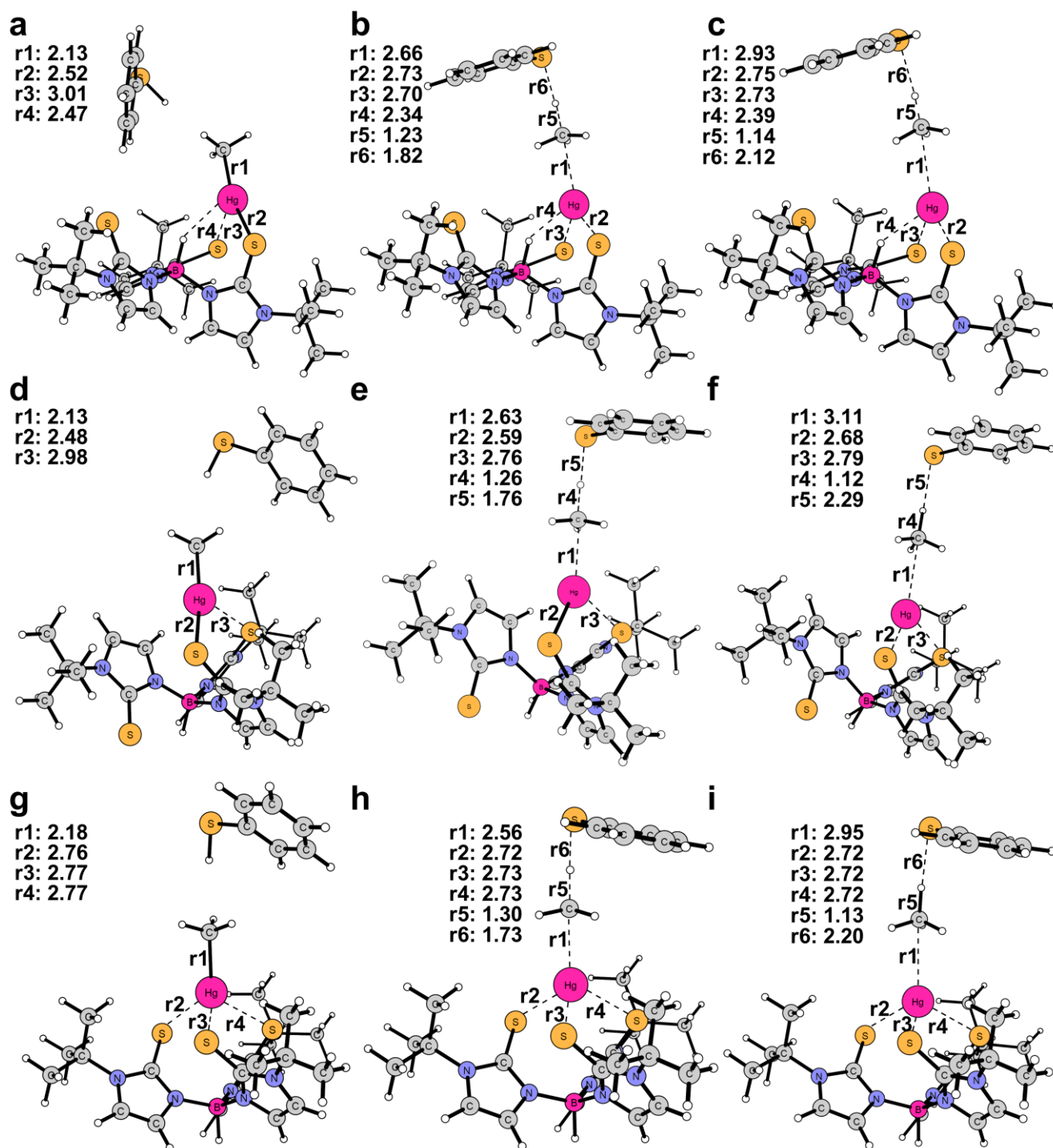


Fig. 4 Structures of the backside attack pathway involving one PhSH molecule. (a), (d), and (g): RE for $[\kappa^1/\kappa^2/\kappa^3\text{-Tm}^t\text{-Bu}]\text{HgMe}$ complexes, respectively. (b), (e), and (h): the corresponding TS. (c), (f), and (i): the corresponding PRO.

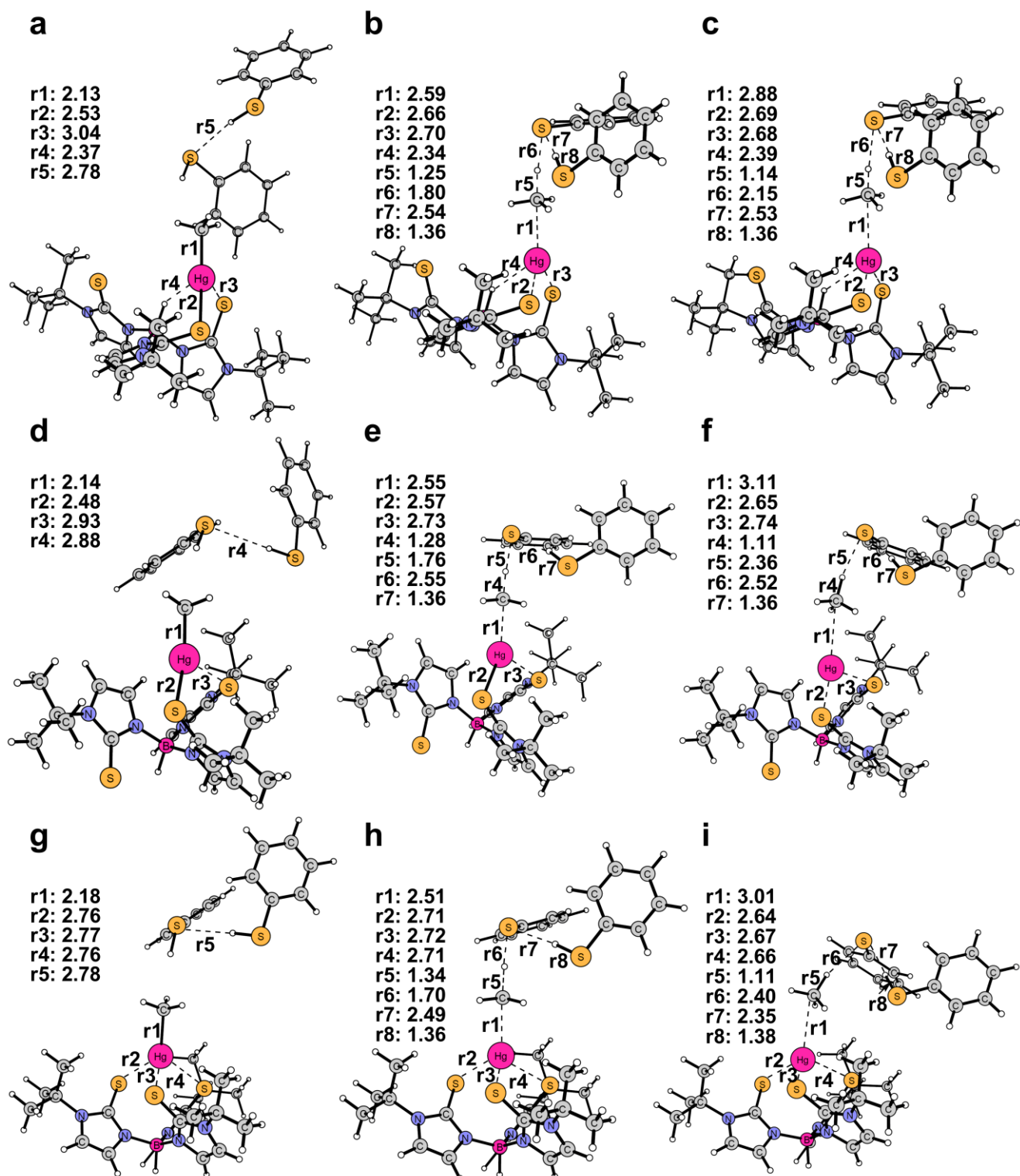


Fig. 5 Structures of the backside attack pathway involving two PhSH molecules. (a), (d), and (g): RE for $[\kappa^1/\kappa^2/\kappa^3\text{-Tm}^{\text{T-Bu}}]\text{HgMe}$ complexes, respectively. (b), (e), and (h): the corresponding TS. (c), (f), and (i): the corresponding PRO.

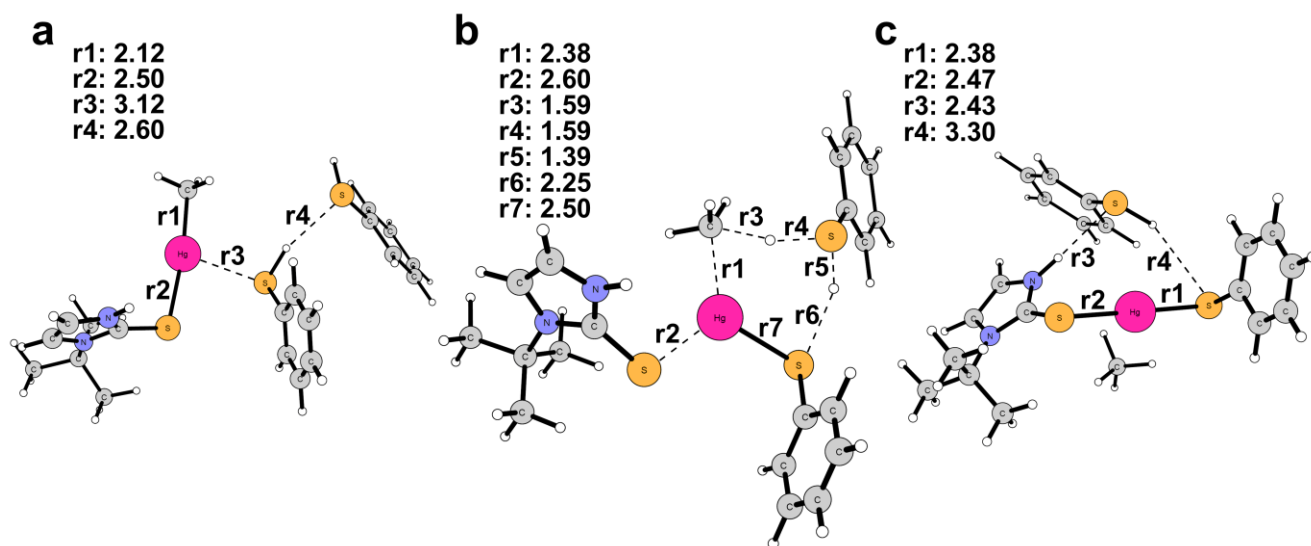


Fig. 6 Structures of the frontside attack pathway featuring six-center TS for $[\text{Hmim}^{\text{t-Bu}}]_{n-1}\text{HgMe}$ complex. (a), (b), and (c): RE, TS, and PRO, respectively.